Applied Physics
Express

LETTER • OPEN ACCESS

Correlation between structural properties and electrochemical proton insertion in (001) VO_2 epitaxial films

To cite this article: Sota Fuji *et al* 2025 *Appl. Phys. Express* **18** 045501

View the article online for updates and enhancements.

You may also like

- Optically pumped GaN-based vertical cavity surface emitting laser with strain-compensated AlGaN/InGaN distributed Bragg reflector
T. Kawashima, M. Kaminishi, C. Kimura et al.

- AlGaN/GaN-based multi-channel epitaxial structure with an ultra-low 2DEG density and superior carrier transport performance
Quan Dai, Qingru Wang, Xinkun Zhang et al.

- Monolithic vertical cavities via selective-area growth using a rotational metal mask and InAs quantum dots for near-infrared multiple-wavelength surface-emitting light source applications
Yuuki C. Hodson, Tatsuki Yokota, Eiichiro Watanabe et al.

This content was downloaded from IP address 130.54.130.253 on 21/04/2025 at 03:11

OPEN ACCESS

Applied Physics Express 18, 045501 (2025) LETTER

https://doi.org/10.35848/1882-0786/adc8f9

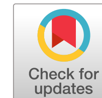

Correlation between structural properties and electrochemical proton insertion in (001) VO_2 epitaxial films

Sota Fuji[1], Yosuke Isoda[1], Xie Lingling[1], Mitsutaka Haruta[1], Takuya Majima[2], Yuichi Shimakawa[1], and Daisuke Kan[1*]

[1]Institute for Chemical Research, Kyoto University, Uji, Kyoto 611-0011, Japan
[2]Department of Nuclear Engineering, Kyoto University, Kyoto 615-8540, Japan

*E-mail: dkan@scl.kyoto-u.ac.jp

Received March 3, 2025; revised March 23, 2025; accepted April 2, 2025; published online April 16, 2025

We epitaxially grew rutile-structured VO_2 films with various out-of-plane lattice constants on (001) TiO_2 substrates by pulsed laser deposition and investigated their protonation by electrochemically injecting protons to the films in transistor structures with gate layers of proton conducting Nafion membranes. We found that VO_2 films with out-of-plane lattice expansion are less protonated. On the basis of the experimental results, we discuss the correlation between the out-of-plane lattice expansion and protonation of (001) VO_2 epitaxial films and highlight that reducing lattice defects is key to promoting the protonation of VO_2 films. © 2025 The Author(s). Published on behalf of The Japan Society of Applied Physics by IOP Publishing Ltd

Supplementary material for this article is available online

Developing solids and artificial structures that can accumulate hydrogen and identifying factors that promote hydrogen accumulation are crucial to both fundamental science and the application of hydrogen to energy devices.[1,2] Moreover, electrochemically accumulating hydrogen into solids or protonation, which results in structural phase changes and electron donation, has been recognized as a way to explore their novel phases with functional properties.[1–6]

Epitaxial films of rutile-structured vanadium dioxide VO_2 have been shown to be protonated by hydrogen-spillover-induced reduction reactions and electrochemical hydrogen injection.[3,7–17] Protonation leads to a two-step transition in VO_2; as protons accumulate, the low-temperature insulating phase first changes to a metallic phase and then the protonation-stabilized metallic phase undergoes a transition to an insulating one. While it has been established that protonation enables the structural and transport properties of VO_2 to be controlled, it remains elusive as to which factors affect and particularly promote protonation processes that are considered to involve proton diffusion in vacancy channels along the c-axis of the rutile structure and bonding to oxygen in VO_2 lattices.[10,12,13,15,18,19] Furthermore, depending on lattice mismatch between the film and substrate and the growth conditions, film lattices often have point defects like oxygen vacancies and lattice deformations that might affect proton diffusion and protonation.[9,20–22] Therefore, key structural factors for protonation remain elusive, and delineating how the structural properties of VO_2 epitaxial films correlate with proton accumulation is needed in order to gain deep insight into protonation processes.

In this study, we grew VO_2 epitaxial thin films with various out-of-plane lattice constants by pulsed laser deposition and investigated the correlations between their structural properties and electrochemical proton accumulation. On the basis of the experimental observations, we discuss key structural factors that affect the protonation of VO_2 epitaxial films.

VO_2 thin films were epitaxially grown on TiO_2(001) single crystal substrates by pulsed laser deposition (PLD). A V_2O_3 pellet, which was prepared with solid-state reactions, was pulsed with a KrF excimer laser ($\lambda = 248$ nm) with a laser spot density of $\sim$1 J cm^{-2} (laser intensity of 120 mJ) and a repetition rate of 5 Hz. The target-to-substrate distance was fixed at $\sim$8 cm. VO_2 epitaxial thin films with thicknesses of 20–50 nm were deposited at substrate temperatures of 350 °C and under oxygen pressures of 8–22 mTorr. The deposition conditions for each sample are shown in Table S1. Figure 1(a) shows X-ray $2\theta/\theta$ patterns around the (002) reflections. All films exhibited (002) Bragg reflections together with clear thickness fringes, which indicated their high quality. While there were some variations in the out-of-plane lattice constants of the fabricated films, the lattice constants were shorter than that of the bulk VO_2 due to the lattice mismatch between TiO_2 and VO_2. Figure 1(b) shows reciprocal space mappings around the (112) TiO_2 reflection for the films with the shortest and longest out-of-plane lattice constants (Samples A and F, respectively). The (112) reflections from the films appear at the same reciprocal-space position along the in-plane direction (Q_{100}) as those of the substrate reflections, indicating that all of the films were fully tensile-strained regardless of their out-of-plane constant. These observations imply that some lattice defects are accommodated in the films due to subtle variations in the deposition conditions, like the deposition temperature and oxygen pressure during deposition, resulting in out-of-plane lattice expansion.

Figure 1(c) shows the temperature dependence of the electrical resistance of Sample A, Sample C, Sample D, and Sample F. The data were obtained using a physical property measurement system (PPMS) by sweeping the temperature from 300 to 250 K, from 250 to 320 K, and then back to 300 K. The resistance changes ΔR due to metal-insulator transitions, which is defined as the ratio of resistances at 250 K and at 300 K (as-grown state), correlated with the films' out-of-plane lattice constants. The film with the shortest out-of-plane lattice constant (Sample A) underwent large ΔR by about three orders of magnitude due to a metal-insulator transition at 287 K. On the other hand, the

Content from this work may be used under the terms of the Creative Commons Attribution 4.0 license. Any further distribution of this work must maintain attribution to the author(s) and the title of the work, journal citation and DOI.

© 2025 The Author(s). Published on behalf of The Japan Society of Applied Physics by IOP Publishing Ltd

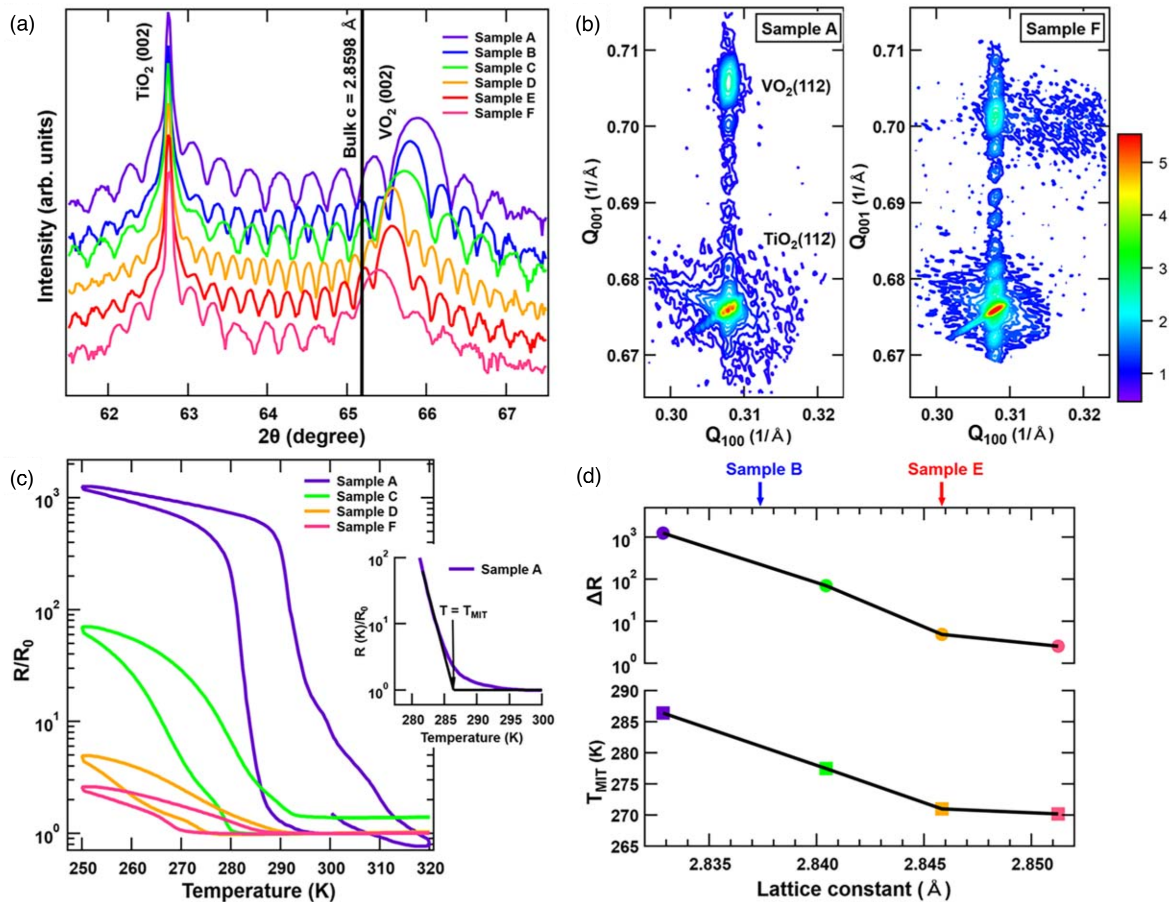

Fig. 1. (a) X-ray $2\theta/\theta$ patterns for (001) VO_2 epitaxial films. (b) Reciprocal space mappings around the (112) reflection for the (001)-oriented VO_2 films (Sample A and Sample F) whose X-ray diffraction patterns are shown in (a). The diffraction intensity is plotted on a logarithmic scale. (c) Temperature dependence of electrical resistance of VO_2 films [Samples A, C, D, and F in (a)]. The resistance of each film is normalized by that of the as-grown state (R_0). The inset shows the definition of the metal-insulator transition temperature T_{MIT}. (d) The magnitude of the resistance change associated with the metal-insulator transition ΔR (upper) and T_{MIT} (bottom) as a function of the out-of-plane lattice constant of (001) VO_2 epitaxial films. The ΔR is defined as the ratio of the resistance at 250 K and R_0, which were measured during the first temperature down sweep.

ΔR and the transition temperature T_{MIT} (definition in the inset) decreased as the out-of-plane lattice constant increased. The correlations between the out-of-plane constant and ΔR and T_{MIT} are highlighted in Fig. 1(d). These observations are consistent with previous studies.[3,23–29] It should be noted that the observed correlation cannot be explained by strain-induced effects,[30–33] which would increase T_{MIT} through lattice expansion along the *c*-axis of the VO_2 lattice. Our observations, therefore, imply that the defects causing the out-of-plane lattice expansion suppress the metal-insulator transition of the VO_2 films and that films with less out-of-plane lattice expansion show a more pronounced transition.

We also found that the out-of-plane lattice expansion is correlated with hydrogen accommodation in the (001) VO_2 epitaxial films. Here, we electrochemically inserted protons into the VO_2 films by employing electric field-effect transistor structures with gate layers of solid-state proton conductor Nafion membranes (Fig. S3). The films were capped with 3 nm thick TiO_2 epitaxial layers grown at a substrate temperature of 350 °C and oxygen partial pressure of 45 mTorr as a protection layer from possible reactions with the Nafion. The transistor structures were fabricated by first sputtering Pt source and drain electrodes (20 nm thick) on the film channels at room temperature and then compressing and bonding the Nafion membranes (Nafion 115, 25 μm in thickness, Sigma Aldrich) to bare VO_2 channel region at 130 °C. The electrochemical proton injection and the resulting reduction reaction in the film channels were induced by applying a gate voltage, V_G, of +3.5 V at 80 °C for 30 min.

Figure 2 summarizes the results for electrochemical hydrogen insertion into Sample B (with the second shortest lattice constant) and Sample E (second longest). Figure 2(a) shows the gate voltage V_G sequence and changes in the resistance during proton injection into the transistor structures at 80 °C. Here, the proton-induced changes in the VO_2 channel resistance were measured at $V_G = 0$ V to avoid possible contamination of the source–drain current by gate leakage current. The resistances of both films increased with the total time of proton injection, indicating that the protons accumulated in the VO_2 lattices and caused non-volatile changes in the resistance. Interestingly, the magnitude of the resistance change depended on the out-of-plane lattice expansion in the VO_2 films. The change in the resistance of Sample B (with the smaller out-of-plane lattice constant) was much larger than that of Sample E. This result implies that more protons accumulate in the lattice of (001) VO_2 films with less out-of-plane lattice expansion and that defects resulting in out-of-plane lattice expansion suppress proton accommodation in VO_2 lattices.

© 2025 The Author(s). Published on behalf of The Japan Society of Applied Physics by IOP Publishing Ltd

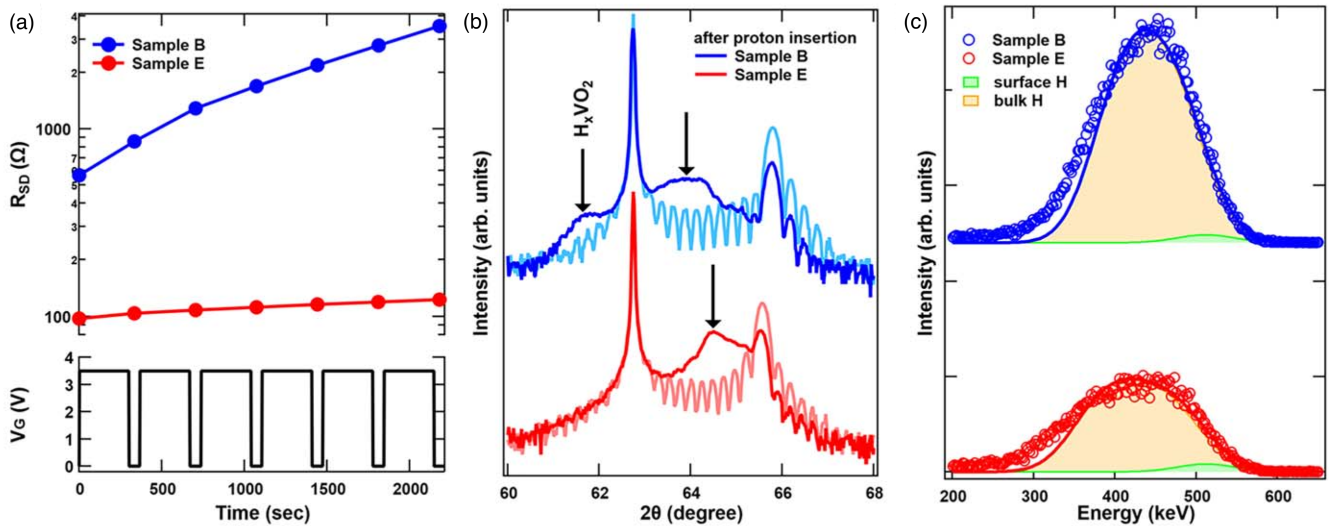

Fig. 2. (a) Changes in the resistance of VO_2 channels (Sample B and Sample E) during proton injection at 80 °C. The bottom panel shows the gate voltage V_g sequence used for the proton injection. The duration of the gate voltage pulses was set to 300 s. The VO_2 channel resistance was measured under $V_g = 0$ V. (b) X-ray $2\theta/\theta$ diffraction patterns for Sample B and Sample E after proton injection at 80 °C ($V_g = 3.5$ V and 30 min). The diffraction patterns were taken at room temperature. For comparison, the diffraction patterns for Sample B and Sample E before proton injection (the as-grown state) are also shown in the light blue and pink lines, respectively. (c) Elastic recoil detection analysis (ERDA) spectra for Sample B and Sample E after proton injection at 80 °C ($V_g = 3.5$ V and 30 min). The spectra were taken at room temperature.

The effect of the out-of-plane lattice expansion on proton accumulation in the VO_2 lattice was further investigated by carrying out an X-ray diffraction characterization and elastic recoil detection analysis (ERDA) for Sample B and Sample E before and after the proton injection process, as shown in Figs. 2(b) and 2(c). These characterizations for films after the proton injection were performed on surfaces exposed by peeling off the Nafion membranes. X-ray diffraction patterns in Fig. 2(b) show that the proton injection decreases the intensity of the (002) VO_2 reflection and results in the additional reflections indicating the protonation of VO_2 films to H_xVO_2. We note that VO_2 films under source and drain electrodes remain unreacted with injected protons. This is part of the reason why the protonated samples exhibit (002) VO_2 reflections. Previous studies have indicated that the out-of-plane lattice constant of a protonated phase (HVO_2) made from (001) VO_2 films was ~3.026 Å (the corresponding 2θ value is 61.21°).[7,9] The H_xVO_2 in Sample B exhibited two reflections. The one at $2\theta \sim 61.65°$ was slightly larger than that of HVO_2 ($x = 1$), while the other at $2\theta \sim 63.93°$ occupied a larger 2θ region compared with the former, implying that the proton concentration of H_xVO_2 in Sample B was less than $x \sim 1$. In addition, the H_xVO_2 reflection in Sample E appeared at a larger 2θ value than in Sample B; thus, Sample E would have been less protonated than Sample B, although they had the same protonation conditions.

We carried out ERDA and examined the concentrations of hydrogen in Sample B and Sample E. The measurements were conducted at the 1.7 MV tandem accelerator facility of the Quantum Science and Engineering Center, Kyoto University. The spectra were obtained with 7.5 MeV Si^{4+} beams incident at an angle of ~75° to the surface normal and by detecting H atoms recoiling from the films at a scattering angle of 30°. The obtained ERDA spectra were simulated and fitted with the SIMNRA 7.03 software. The spectra for the protonated Samples B and E and their fitting results are shown in Fig. 2(c). The plot shows a broad peak that can be accounted for by assuming two contributions: H adsorbed on the VO_2 surfaces (~510 keV, referred to as surface H) and H in the bulk film (~450 keV, referred to as bulk H). Bulk H made a much larger contribution to the spectrum of Sample B than to Sample E. The fitting results indicated that the H concentrations (per VO_2 formula unit) were 0.51 in Sample B and 0.22 in Sample E. These values are in accord with expectations from the XRD measurement results in Fig. 2(b). It is worthwhile pointing out that as shown in Fig. S4, accumulating a small amount of proton (like in Sample E and Sample F) lowers the metal-insulator transition temperature and stabilizes the metallic phase of VO_2, which is consistent with the previous reports [Refs. 7, 11]. This primarily explains why the resistance difference by several tens of times were seen between the protonated Sample B and Sample E (and F) even though the proton concentration of Sample B is larger only by a factor of two to three than that of Sample E. Our results indicate that defects and dislocations expanding VO_2 lattices suppress proton insertion and that VO_2 films with fewer defects, and thus shorter out-of-plane lattice constants, can accommodate large amounts of hydrogen.

To obtain more insight into lattice defects that suppress the protonation in VO_2 lattices, we carried out cross-sectional (scanning) transmission electron microscopy ((S)TEM) observations and electron energy loss spectroscopy (EELS) characterizations on samples that had out-of-plane lattice constants very close to those of Sample B and Sample E. Cross-sectional TEM samples were prepared by a focused ion-beam system (Hitachi NX5000). TEM and STEM experiments were conducted at room temperature by JEM-ARM200F with an EELS spectrometer (Gatan Quantum ERS). The acceleration voltage was 200 kV. In STEM-EELS experiments, the probe convergence semi-angle was 24.6 mrad, and the EELS collection semi-angle was 57.3 mrad. EELS spectra were obtained in dual EELS mode. The results are summarized in Fig. 3. While the

© 2025 The Author(s). Published on behalf of The Japan Society of Applied Physics by IOP Publishing Ltd

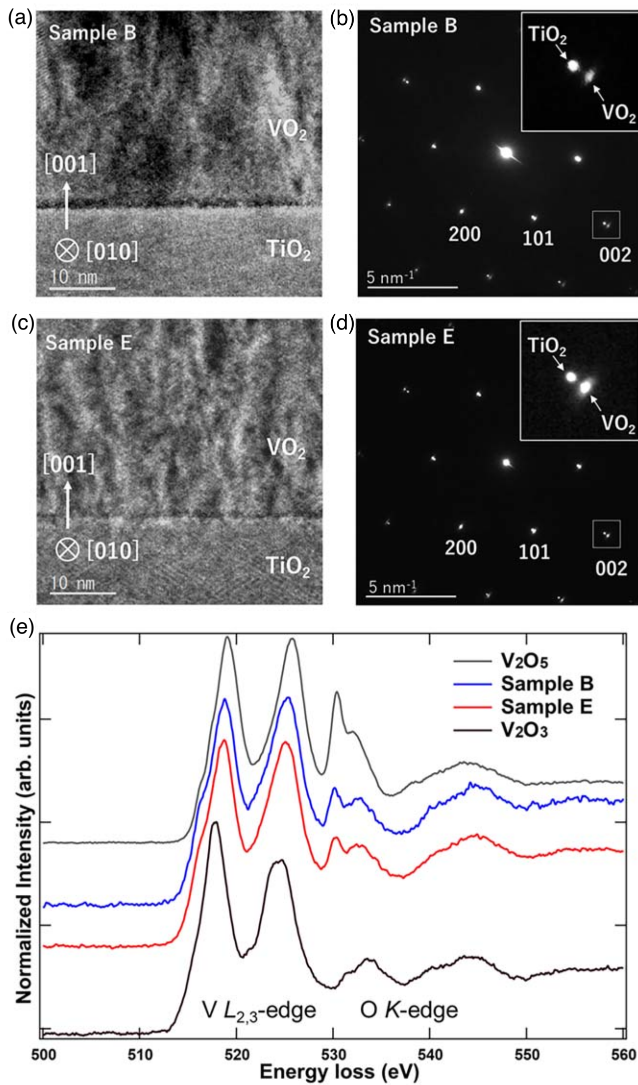

Fig. 3. (a), (b) Cross-sectional TEM images and (c), (d) electron diffraction patterns for Sample B and Sample E. The insets of (c), (d) are enlarged views of the (002) diffraction spots of VO_2 films and TiO_2 substrates. (e) Electron energy loss spectroscopy (EELS) spectra of V L-edge and O K-edge for Sample B and Sample E. The spectra of reference powder samples of V_2O_3 and V_2O_5 are shown for comparison.

interfaces between VO_2 films and TiO_2 substrates are apparently sharp in both samples, film regions with homogeneous image contrast are much wider in Sample B than in Sample E [Figs. 3(a), 3(c), and S1]. In addition, as shown in Figs. 3(b) and 3(d), diffraction spots from the VO_2 region of Sample E are elongated along the [100] direction. These observations imply that Sample E had more defects and dislocations, with a larger out-of-plane lattice expansion, compared with Sample B. Figure 3(e) shows EELS spectra around the V $L_{2,3}$-edge and O K-edge from Sample B and Sample E, together with spectra of reference powder samples of $V^{3+}{}_2O_3$ and $V^{5+}{}_2O_5$. The peak positions of the V $L_{2,3}$-edge spectra for Sample B and Sample E are essentially the same, and their peaks are at larger energy-loss values than those of $V^{3+}{}_2O_3$ and smaller values than those of $V^{5+}{}_2O_5$. These observations imply that the V valence states in the VO_2 film regions of the films are essentially the same regardless of the films' out-of-plane lattice expansion, ruling out the possibility that oxygen vacancies, which would lead to a reduction in the V valence state, have the primary influence on the lattice expansion and protonation in the VO_2 lattices investigated in this study. If oxygen vacancies were at play and promoted proton diffusion in oxide lattices,[10] the VO_2 films with expanded out-of-plane lattice constants and suppressed metal-insulator transitions would be more protonated. Such an expectation is opposite to what we experimentally observed. Therefore, the suppressed protonation of the VO_2 films with out-of-plane lattice expansion is probably related to lattice defects like stacking faults rather than point defects like oxygen vacancies.

It should be noted that the rutile structure of MO_2 (M: transition metals) consists of oxygens arranged in (distorted) hexagonal-close-packed (h.c.p.) array and cations occupying half of the octahedral sites in the h.c.p. oxygen array, as shown in Fig. S2. We think that (001) VO_2 films with out-of-plane lattice expansion (for example, Sample E and Sample F) should have more disorder in V occupation at the octahedral sites of the h.c.p. oxygen array (a mixture of type-A and type-B occupations in Fig. S2). Such disorder in VO_2 lattices would make the in-plane grain size small and block vacancy channels along the c-axis, and as a result, proton diffusion along the channels and protonation would be suppressed, which explains why VO_2 films that undergo lattice expansion are less protonated.

In summary, we investigated the protonation of rutile-structured (001) VO_2 epitaxial films with various out-of-plane lattice constants and revealed the correlation between the out-of-plane lattice expansion and protonation of the VO_2 epitaxial films. We showed that VO_2 films with out-of-plane lattice expansion have large numbers of defects that block the vacancy channels and that the defects result from the disordered occupation of V in the octahedral sites of the h.c.p. oxygen array. These findings explain why the protonation of the films with out-of-plane lattice expansion is suppressed. Our study indicates that reducing such lattice defects in VO_2 films is key to promoting their protonation.

Acknowledgments We thank Mr Keitaro Watanabe and Mr Keisuke Igarashi (Hitachi High-Tech Corporation) for fabricating the TEM samples by FIB. This work was partly supported by Grants-in-Aid for Scientific Research (No. 21H01810, 22H04617, 23KJ1239, 23H04110, 23H05457, and 24KJ1371) and by grants for the Integrated Research Consortium on Chemical Sciences and the International Collaborative Research Program of the Institute for Chemical Research in Kyoto University from the Ministry of Education, Culture, Sports, Science, and Technology (MEXT) of Japan. The work was also supported by JST SPRING, Grant No. JPMJSP2110, and the Japan Science and Technology Agency (JST) as part of PRESTO, Grant No. JPMJPR24H3 and the Adopting Sustainable Partnerships for Innovative Research Ecosystem (ASPIRE), Grant Nos. JPMJAP2312 and JPMJAP2314.

ORCID iDs Yosuke Isoda https://orcid.org/0000-0003-4445-9908 Mitsutaka Haruta https://orcid.org/0000-0002-2237-7242 Takuya Majima https://orcid.org/0000-0003-2804-1915 Yuichi Shimakawa https://orcid.org/0000-0003-1019-2512 Daisuke Kan https://orcid.org/0000-0002-7505-0059

1) C. Leighton, Nat. Mater. **18**, 13 (2019).
2) Y. Guan, H. Han, F. Li, G. Li, and S. Parkin, Annu. Rev. Mater. Res. **53**, 25 (2023).
3) J. Jeong, N. Aetukuri, T. Graf, T. D. Schladt, M. G. Samant, and S. S. P. Parkin, Science **339**, 1402 (2013).
4) N. Lu et al., Nature **546**, 124 (2017).
5) M. Li, W. Han, X. Jiang, J. Jeong, M. G. Samant, and S. S. P. Parkin, Nano Lett. **13**, 4675 (2013).
6) H. T. Yi, B. Gao, W. Xie, S.-W. Cheong, and V. Podzorov, Sci. Rep. **4**, 6604 (2014).
7) H. Yoon, M. Choi, T.-W. Lim, H. Kwon, K. Ihm, J. K. Kim, S.-Y. Choi, and J. Son, Nat. Mater. **15**, 1113 (2016).
8) K. Shibuya and A. Sawa, Adv. Electron. Mater. **2**, 1500131 (2016).

© 2025 The Author(s). Published on behalf of
The Japan Society of Applied Physics by IOP Publishing Ltd

9) H. Yoon, J. Park, S.-Y. Choi, D. Lee, and J. Son, Adv. Electron. Mater. **4**, 1800128 (2018).
10) C. Oh, I. Kim, J. Park, Y. Park, M. Choi, and J. Son, Adv. Electron. Mater. **7**, 2000802 (2021).
11) M. Jo, H. J. Lee, C. Oh, H. Yoon, J. Y. Jo, and J. Son, Adv. Funct. Mater. **28**, 1802003 (2018).
12) K. Muraoka and T. Kanki, Sci. Rep. **9**, 20093 (2019).
13) Y. Cai, Z. Wang, J. Wan, J. Li, R. Guo, J. W. Ager, A. Javey, H. Zheng, J. Jiang, and J. Wu, Nat. Commun. **15**, 5814 (2024).
14) S. Chen, Z. Wang, H. Ren, Y. Chen, W. Yan, C. Wang, B. Li, J. Jiang, and C. Zou, Sci. Adv. **5**, eaav6815 (2019).
15) J. Jeong, N. B. Aetukuri, D. Passarello, S. D. Conradson, M. G. Samant, and S. S. P. Parkin, Proc. Natl. Acad. Sci. USA **112**, 1013 (2015).
16) D. Passarello, S. G. Altendorf, J. Jeong, M. G. Samant, and S. S. P. Parkin, Nano Lett. **16**, 5475 (2016).
17) S. Chen, X. J. Wang, L. Fan, G. Liao, Y. Chen, W. Chu, L. Song, J. Jiang, and C. Zou, Adv. Funct. Mater. **26**, 3532 (2016).
18) J. Lin, H. Ji, M. W. Swift, W. J. Hardy, Z. Peng, X. Fan, A. H. Nevidomskyy, J. M. Tour, and D. Natelson, Nano Lett. **14**, 5445 (2014).
19) A. Pofelski, H. Jia, S. Deng, H. Yu, T. J. Park, S. Manna, M. K. Y. Chan, S. K. R. S. Sankaranarayanan, S. Ramanathan, and Y. Zhu, Nano Lett. **24**, 1974 (2024).
20) Y. Isoda, T. N. Pham, R. Aso, S. Nakamizo, T. Majima, S. Hosokawa, K. Nitta, Y. Morikawa, Y. Shimakawa, and D. Kan, Nat. Commun. **16**, 56 (2025).
21) Y. Isoda, D. Kan, T. Majima, and Y. Shimakawa, Appl. Phys. Express **16**, 015506 (2023).
22) J. Park, H. Yoon, H. Sim, S.-Y. Choi, and J. Son, ACS Nano **14**, 2533 (2020).
23) Z. Zhang et al., Phys. Rev. Appl. **7**, 034008 (2017).
24) A. Moatti, R. Sachan, and J. Narayan, J. Appl. Phys. **128**, 045302 (2020).
25) A. Moatti, R. Sachan, S. Gupta, and J. Narayan, ACS Appl. Mater. Interfaces **11**, 3547 (2019).
26) Y. Park et al., Nat. Commun. **11**, 1401 (2020).
27) D. Lee et al., Science **362**, 1037 (2018).
28) J. Zhang, Z. Zhao, J. Li, H. Jin, F. Rehman, P. Chen, Y. Jiang, C. Chen, M. Cao, and Y. Zhao, ACS Appl. Mater. Interfaces **9**, 27135 (2017).
29) Q. Lu et al., Sci. Rep. **10**, 18554 (2020).
30) N. B. Aetukuri et al., Nat. Phys. **9**, 661 (2013).
31) Y. Muraoka, Y. Ueda, and Z. Hiroi, J. Phys. Chem. Solids **63**, 965 (2002).
32) K. Nagashima, T. Yanagida, H. Tanaka, and T. Kawai, J. Appl. Phys. **100**, 063714 (2006).
33) J. Cao et al., Nano Lett. **10**, 2667 (2010).

© 2025 The Author(s). Published on behalf of
The Japan Society of Applied Physics by IOP Publishing Ltd